

On the Application of AERONET-OC Multispectral Data to Assess Satellite-Derived Hyperspectral R_{rs}

Marco Talone[✉], Senior Member, IEEE, Giuseppe Zibordi[✉], and Jaime Pitarch[✉]

Abstract—The potential for applying in situ multispectral R_{rs} data from the Ocean Color component of the Aerosol Robotic Network (AERONET-OC) to validate satellite-derived ocean color hyperspectral R_{rs} products was investigated in the 400–700 nm interval. The analysis was performed using a comprehensive dataset of simulated hyperspectral R_{rs} in combination with an algorithm designed to reconstruct hyperspectral R_{rs} from multispectral ones. Results were assessed using in situ hyperspectral R_{rs} representative of diverse water types. Excluding waters dominated by a high concentration of colored dissolved organic matter, results indicate the capability of determining hyperspectral R_{rs} from AERONET-OC multispectral data with mean relative and absolute uncertainties generally lower than 2% and $5 \times 10^{-5} \text{ sr}^{-1}$, respectively, at a number of the key center-wavelengths of the Ocean Color Instrument (OCI) onboard the Plankton, Aerosol, Cloud, ocean Ecosystem (PACE) spacecraft.

Index Terms—Ocean color, remote sensing, validation.

I. INTRODUCTION

SATELLITE-DERIVED remote sensing reflectance R_{rs} of natural waters has shown fundamental relevance to investigate marine ecosystems through retrieved information on optically significant water constituents such as phytoplankton concentration. This was achieved through multispectral data across a number of satellite sensor including the Sea-viewing Wide Field-of-view Sensor (SeaWiFS [1]) up to the recent Ocean and Land Color Instrument (OLCI [2]).

Further advances in satellite ocean color applications, likely benefitting of a robust determination and quantification of phytoplankton species, are expected by the exploitation of data from hyperspectral sensors like those operated by the Italian Space Agency on the PRcursore IperSpettrale della Missione Applicativa (PRISMA) [3] or by the National Aeronautics and

Manuscript received 20 October 2023; accepted 3 January 2024. Date of publication 8 January 2024; date of current version 22 January 2024. This work was supported in part by the “Severo Ochoa Center of Excellence” Accreditation under Grant CEX2019-000928-S and in part by the National Aeronautics and Space Administration (NASA) through the Goddard Earth Sciences Technology and Research (GESTAR) II Award under Grant 80NSSC22M0001. The work of Jaime Pitarch was supported by the European Union through the NextGenerationEU Program, Italian Integrated Environmental Research Infrastructures System (ITINERIS) Project. (Corresponding author: Marco Talone.)

Marco Talone is with the Departament de Oceanografia Física i Tecnològica and the Barcelona Expert Center (BEC), Institut de Ciències del Mar (ICM-CSIC), 08003 Barcelona, Spain (e-mail: talone@icm.csic.es).

Giuseppe Zibordi is with the Goddard Space Flight Center, National Aeronautics and Space Administration, Greenbelt, MD 20771 USA, and also with the Southeastern Universities Research Association, Washington, DC 20005 USA.

Jaime Pitarch is with the Istituto di Scienze Marine, Consiglio Nazionale delle Ricerche (ISMAR-CNR), 00133 Rome, Italy.

Digital Object Identifier 10.1109/LGRS.2024.3350928

Space Administration on the forthcoming Plankton, Aerosol, Cloud, ocean Ecosystem (PACE) [4].

The increased spectral resolution and number of satellite sensors bands, however, require adequate in situ reference measurements for a comprehensive validation of derived radiometric data products. This implies access not only to in situ measurements exhibiting suitable spatio-temporal coverage, but also satisfying the uncertainty requirements allowing to verify the fitness-for-purpose of satellite-derived radiometric products at the relevant center-wavelengths. This need urges advancements on those satellite validation methods still relying on multispectral data such as those from the Ocean Color component of the Aerosol Robotic Network (AERONET-OC) [5]. As an alternative to the exclusive use of hyperspectral sensor data (e.g., those from WATER-HYPERNET [6]) to support the validation of satellite hyperspectral radiometric products, this work addresses the potential for applying multispectral data without restricting the process to the sole matching spectral bands. This effort is justified by: 1) the evidence that a finite number of spectral R_{rs} values allows for reconstructing the full R_{rs} spectrum, still at the expense of a decreased accuracy (e.g., [7], [8]); 2) the assumption that a relatively small increase in the uncertainty of reconstructed R_{rs} values away from the actual in situ center-wavelengths might still ensure basis for a satisfactory exploitation of these data in the validation of satellite ocean color radiometric products; and 3) the outstanding maturity of the AERONET-OC network that, established in 2002, benefits of high standardization of instruments and measurement methods [5], unique investigations on instruments performance [9] and measurement uncertainties [10], extensive efforts to verify the accuracy of radiometric products [11], and consolidated data reduction and quality control schemes [12].

The main objective of the study is the quantification of the uncertainties characterizing reconstructed R_{rs} at PACE ocean color center-wavelengths solely relying on AERONET-OC multispectral data from diverse water types.

II. DATA AND METHODS

A. R_{rs} Center-Wavelengths

In agreement with the objective of the work, R_{rs} spectral values at the center-wavelengths of the Ocean Color Instrument (OCI) onboard PACE, were determined exclusively using R_{rs} values at the AERONET-OC marine center-wavelengths in the visible spectral region [5]. For the sake of simplicity, bandwidths and spectral response functions were neglected.

TABLE I

CENTER-WAVELENGTHS CONSIDERED IN THIS STUDY: THE SUPERSCRIPTS i AND s GENERICALLY INDICATE THE IN SITU AND SATELLITE CENTER-WAVELENGTHS, RESPECTIVELY, WHILE THE SUBSCRIPTS n AND m IDENTIFY THE RELATED SPECTRAL BANDS

	Center-wavelengths [nm]
AERONET-OC (λ_n^i)	400, 412.5, 442.5, 490, 510, 560, 620, 665
PACE- h (λ_m^s)	Assumed to have a 5 nm regular grid in the 400–700 nm spectral interval
PACE- m (λ_m^s)	412, 425, 443, 460, 475, 490, 510, 532, 555, 583, 617, 640, 655, 665

It is recognized that this may affect the accuracy of results, however, the impact is assumed minor with respect to ignoring inaccuracies introduced by significant spectral mismatches.

The center-wavelengths considered in this study are summarized in Table I: the nominal AERONET-OC center-wavelengths in the 400–665 nm range supporting marine applications; a 5 nm regular grid between 400 and 700 nm expected to mimic PACE-OCI full resolution visible center-wavelengths (PACE- h); and a sub-set of the PACE-OCI center-wavelengths in the 412–665 nm interval considered of major interest for ocean color applications (PACE- m) [13].

B. Experimental and Simulated Datasets

The in situ hyperspectral radiometric measurements supporting the assessment of the scheme applied for the reconstruction of R_{rs} spectra, were collected in Mediterranean Sea and Black Sea regions characterized by water types varying from oligotrophic to optically complex. Measurements were performed using TriOS (Rastede, Germany) RAMSES radiometers exhibiting nominal spectral range of 320–950 nm, sampling of 3.3 nm, and resolution of approximately 10 nm. The radiometers were operated on a towed floating frame named Optical Floating System (OFS) [14]. Each OFS measurement sequence comprised successive acquisitions of simultaneous subsurface nadir upwelling radiance L_u and of above water downward irradiance E_d . RAMSES data were calibrated and processed to produce R_{rs} spectra with a regular spectral sampling of 2 nm in the 400–700 nm spectral interval (see details in [14]). For each spectrum, the water type of pertinence was determined in agreement with its spectral shape: Case-1 waters with optical properties solely determined by phytoplankton, here identified by R_{rs} maxima below 450 nm; Case-2a waters characterized by moderate to high concentrations of suspended sediments, identified by R_{rs} maxima in the 450–550 nm spectral interval; and Case-2b waters with high concentration of chromophoric dissolved organic matter (CDOM), identified by R_{rs} maxima beyond 550 nm. The geographic locations of measurements and the related R_{rs} spectra, are displayed in Fig. 1.

A dataset of simulated R_{rs} spectra [15] representative of clear sky and of homogeneous and infinitely deep sea, is used to support the reconstruction of hyperspectral R_{rs} from multispectral ones. The dataset, which includes approximately 5000 R_{rs} spectra with 1 nm resolution, was constructed using Hydrolight (Sequoia Scientific, Inc., Bellevue, WA, USA) with input chlorophyll concentration, nonalgal particles concentration, and absorption of colored dissolved organic matter at 440 nm, determined using experimental biooptical

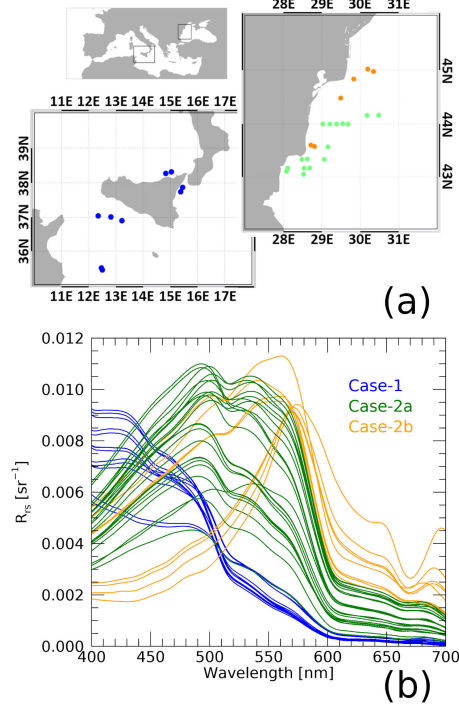


Fig. 1. (a) Geographic location of measurements and (b) corresponding in situ hyperspectral R_{rs} . Measurements performed in Case-1, -2a, and -2b waters are displayed in blue, green, and orange, respectively (redrawn from [14]).

relationships encompassing oceanic, turbid coastal, eutrophic, and CDOM-dominated waters. The angular scattering was modeled with Fournier-Forand phase functions for phytoplankton and nonalgal particles. Inelastic scattering was neglected.

C. Reconstruction of Hyperspectral R_{rs}

The determination of hyperspectral R_{rs} from multispectral ones is here inspired to the general principles introduced in previous studies investigating the accuracy of reconstructed spectra as a function of the number of spectral bands [7], [8].

By relying on multispectral R_{rs} extracted from in situ hyperspectral data (i.e., TriOS derived R_{rs}) at the specific AERONET-OC marine center-wavelengths λ_n^i and additionally benefiting of simulated hyperspectral remote sensing reflectances R_{rs}^{ref} , the reconstruction of hyperspectral spectra from the multispectral ones, encompassed the following steps.

- 1) The Euclidean distance d between in situ and simulated spectra was computed with

$$d = \sqrt{\sum_{\lambda_n^i} (R_{rs}(\lambda_n^i) - R_{rs}^{\text{ref}}(\lambda_n^i))^2} \quad (1)$$

by considering the sole center-wavelengths λ_n^i in the 400–620 nm interval.

- 2) The three simulated spectra R_{rs}^{sel} exhibiting the lowest distances d were selected.
- 3) The coefficient $k(\lambda_n^i)$ was computed as

$$k(\lambda_n^i) = R_{rs}(\lambda_n^i) \times [\text{avg}(R_{rs}^{sel}(\lambda_n^i))]^{-1} \quad (2)$$

where $\text{avg}(R_{rs}^{sel}(\lambda_n^i))$ is the average of the selected R_{rs}^{sel} spectra at each λ_n^i .

- 4) Finally, the remote sensing reflectance $\hat{R}_{rs}(\lambda_m^s)$ at any center-wavelengths λ_m^s was calculated as

$$\hat{R}_{rs}(\lambda_m^s) = k(\lambda_m^s) \times \text{avg}(R_{rs}^{sel}(\lambda_m^s)) \quad (3)$$

where the coefficient $k(\lambda_m^s)$ was determined for each λ_m^s by linearly interpolating the $k(\lambda_n^i)$ values.

D. Metrics to Assess the Accuracy of Reconstructed Spectra

The performance of the reconstruction process was assessed using differences between reconstructed satellite $\hat{R}_{rs}(\lambda_m^s)$ (as obtained from $R_{rs}(\lambda_n^i)$ applying Eq. 3) and actual in situ hyperspectral R_{rs} . Specifically, relative $\varepsilon(\lambda_m^s)$ and absolute $\Delta(\lambda_m^s)$ differences were determined at the satellite center-wavelengths λ_m^s as

$$\varepsilon(\lambda_m^s) = 100 \times \left[\frac{\hat{R}_{rs}(\lambda_m^s) - R_{rs}(\lambda_m^s)}{R_{rs}(\lambda_m^s)} \right] \quad (4)$$

and

$$\Delta(\lambda_m^s) = \hat{R}_{rs}(\lambda_m^s) - R_{rs}(\lambda_m^s). \quad (5)$$

III. RESULTS

Results from assessments performed for each water type are summarized in Table II for the PACE-*m* center-wavelengths and additionally displayed in Fig. 2 for both the PACE-*m* and PACE-*h* ones.

The largest mean relative differences are generally observed in regions characterized by ample spectral gradients of R_{rs} ; around 600 nm regardless of the water type, and around 530 nm for Case-2b water spectra. When restricting the analysis to the PACE-*m* center-wavelengths, the mean relative spectral differences $\text{avg}(\varepsilon)$ between reconstructed and actual in situ R_{rs} are generally within $\pm 2\%$ for Case-1 and Case-2a water spectra, but still reach 3%–4% at 640 and 655 nm. Case-2b water spectra exhibit relatively high values of $\text{avg}(\varepsilon)$ approaching 4% at 640 nm and 5% at 532 nm. The large mean relative differences are generally associated with ample $\text{std}(\varepsilon)$.

The mean absolute differences $\text{avg}(\Delta)$ at the PACE-*m* center-wavelengths show typical values ranging from approximately $5 \times 10^{-5} \text{ sr}^{-1}$ for Case-1 water spectra up to more than $20 \times 10^{-5} \text{ sr}^{-1}$ for Case-2b water spectra.

To comprehensively support the application of in situ data to the validation of satellite data products, the uncertainties due to the reconstruction process have been evaluated. Specifically, the associated relative u_r and absolute u_a uncertainties have been estimated through the root mean square of the ε and Δ values, respectively. Results are displayed

in Fig. 3 as a function of the water type, with the errorbars indicating the precision characterizing the $\text{avg}(R_{rs}^{sel})$ reference spectra, computed as the average of the standard deviations of the R_{rs}^{sel} spectra, scaled by the square root of their number.

With reference to the relative uncertainties u_r , these show a significant dependence with wavelength across all water types. At the PACE-*m* center-wavelengths, Case-1 and Case-2a water spectra show values of u_r generally lower than 2% up to 560 nm, while they can reach 3%–4% beyond such a wavelength. Case-2b water spectra show u_r values exceeding 2% also at 460, 475, and 532 nm.

Absolute uncertainties u_a exhibit spectral features depending on water type. Case-1 water spectra show values of u_a generally lower than $5 \times 10^{-5} \text{ sr}^{-1}$. Conversely, Case-2a and Case-2b water spectra may display much larger values (see Fig. 3).

IV. DISCUSSION

Results from the above analyses confirm the potential for applying in situ multispectral R_{rs} data to validate satellite derived hyperspectral radiometric products at the expense of unavoidable uncertainties due to the reconstruction of spectra. In fact, when the uncertainty contribution due to the reconstruction is constrained below approximately 1%–2%, it can be assumed to not largely affect the uncertainty budget characterizing radiometric data products (e.g., see [10]).

The study confidently opens to the assessment of PACE-OCI derived R_{rs} at center-wavelengths of major interest for the ocean color community through the use of AERONET-OC multispectral data. This naturally allows for benefitting from a number of globally distributed measurement sites embracing very diverse water types with exceptional seasonal and multiannual temporal coverage.

Overall results suggest a better performance of the reconstruction process for data from AERONET-OC sites located in oligotrophic/mesotrophic waters (i.e., Case-1) such as the Casablanca Platform in the western Mediterranean Sea, or in optically complex waters with varying concentrations of sediments and CDOM (i.e., Case-2a) such as the Acqua Alta Oceanographic Tower (AAOT) in the northern Adriatic Sea or, Section-7 and Galata in the Black Sea. Less promising appears the exploitation of AERONET-OC data from CDOM dominated waters (i.e., Case-2b) such as Irbe Lighthouse or Gustaf Dalen Lighthouse Tower in the Baltic Sea due to uncertainties exceeding 2% in several portions of the visible spectrum.

Definitively, the accuracy of reconstructed spectra depends on: 1) the number and distribution of the spectral bands characterizing the in situ multispectral data and 2) the actual global representativity of the simulated hyperspectral data applied in the re-construction process. This suggests that a reduction of uncertainties is likely achievable not only by expanding the simulated dataset, but also through in situ multispectral data benefitting of an extended number of spectral bands. In particular, the addition of a spectral band at approximately 530 nm would allow reducing below 2% the uncertainties due to reconstruction also for Case-2b water spectra in the

TABLE II
MEAN VALUES AND STANDARD DEVIATIONS OF RELATIVE AND ABSOLUTE DIFFERENCE BETWEEN RECONSTRUCTED AND ACTUAL IN SITU R_{rs} AT THE PACE-*m* CENTER-WAVELENGTHS

λ^s	nm	412	425	443	460	475	490	510	532	555	583	617	640	655	665
Case-1															
$avg(\varepsilon)$	%	-0.06	0.64	-0.01	-0.29	-0.16	0.00	-0.00	-0.29	-1.63	1.13	0.38	4.17	2.83	-0.55
$std(\varepsilon)$	%	0.03	0.28	0.03	0.57	0.80	0.00	0.00	1.24	0.65	2.73	4.10	12.03	10.29	3.11
$avg(\Delta)$	$10^{-5} sr^{-1}$	-0.49	4.68	-0.08	-1.71	-0.62	0.00	-0.00	-1.09	-3.13	0.98	0.17	0.93	0.64	-0.08
$std(\Delta)$	$10^{-5} sr^{-1}$	0.22	1.90	0.17	3.59	4.68	0.00	0.00	3.39	1.75	2.25	1.20	2.55	2.01	0.52
Case-2a															
$avg(\varepsilon)$	%	0.06	0.13	-0.05	-1.21	-0.30	-0.00	0.00	-1.13	-2.02	0.12	1.23	3.14	2.85	0.23
$std(\varepsilon)$	%	0.05	0.35	0.04	0.73	0.89	0.00	0.00	0.66	0.27	1.19	1.44	1.20	1.80	0.64
$avg(\Delta)$	$10^{-5} sr^{-1}$	0.32	0.77	-0.37	-8.67	-2.16	-0.00	0.00	-8.01	-13.43	-0.08	1.87	4.17	3.36	0.25
$std(\Delta)$	$10^{-5} sr^{-1}$	0.28	2.21	0.33	5.39	7.68	0.00	0.00	4.67	4.63	5.20	1.80	2.25	2.34	0.52
Case-2b															
$avg(\varepsilon)$	%	-0.04	-0.63	-0.20	1.27	0.15	0.00	0.00	5.39	0.08	-2.55	-0.68	3.89	0.30	0.26
$std(\varepsilon)$	%	0.09	0.67	0.11	3.02	2.90	0.00	0.00	4.57	1.78	1.60	1.05	1.67	1.95	0.60
$avg(\Delta)$	$10^{-5} sr^{-1}$	-0.06	-2.00	-0.76	3.35	0.52	0.00	0.00	35.27	-1.03	-20.65	-3.14	11.24	-0.25	0.64
$std(\Delta)$	$10^{-5} sr^{-1}$	0.28	1.53	0.29	9.91	9.63	0.00	0.00	24.96	15.78	13.10	4.06	4.75	6.57	1.29

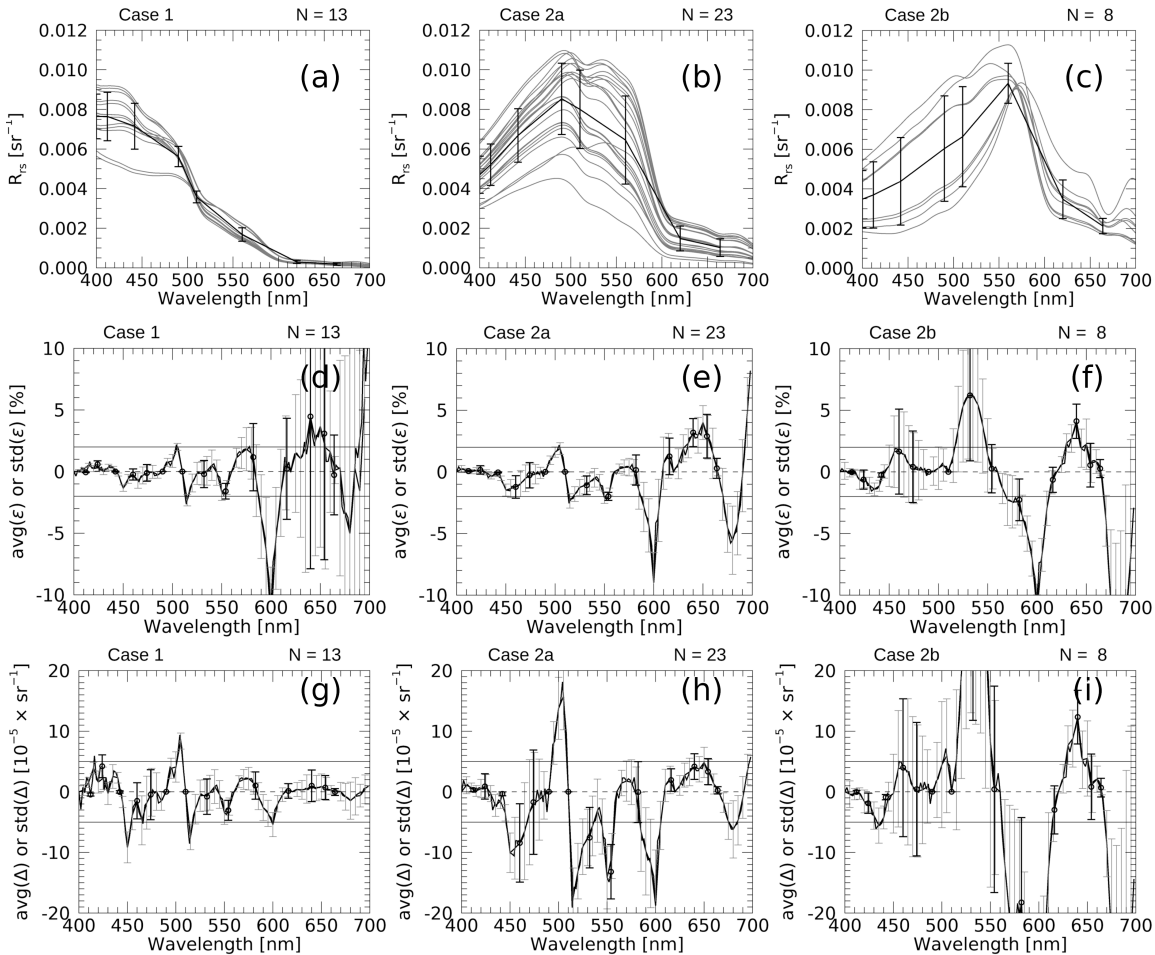


Fig. 2. (a)–(c) R_{rs} spectra included in evaluation, (d)–(f) relative (ε), and (g)–(i) absolute (Δ) differences between reconstructed and actual in situ values for the various water types. The thick lines and the error bars in the upper row indicate the mean values and the standard deviations of R_{rs} at the AERONET-OC center-wavelengths. Error bars in the middle and bottom rows indicate the mean values and standard deviations of the relative and absolute differences determined at the PACE-*h* (gray) and the PACE-*m* (black) center-wavelengths. The solid horizontal lines indicate $\varepsilon = \pm 2\%$ in (d)–(f), and $\Delta = \pm 5 \times 10^{-5} sr^{-1}$ in (g)–(i).

520–550 nm spectral region. Conversely, the addition of a single spectral band at approximately 600 nm does not appear to provide any benefit, regardless of the water type.

It is finally emphasized that the above findings and conclusions should not take away relevance to hyperspectral radiometry, which should remain the favorable source of

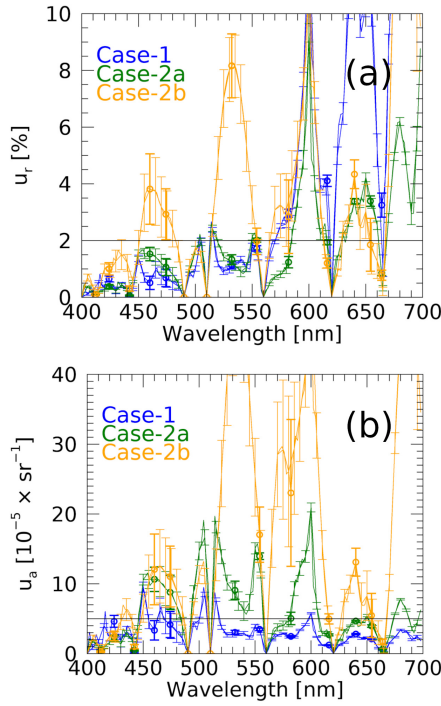


Fig. 3. (a) Relative and (b) absolute uncertainties resulting from the reconstruction of hyperspectral R_{rs} using multispectral values at the AERONET-OC visible center-wavelengths. Thin lines and circles refer to the PACE-*h* and PACE-*m* center-wavelength arrays. Results for Case-1, -2a, and -2b water types are displayed in blue, green, and orange, respectively. The solid horizontal lines indicate $u_r = 2\%$ in (a), and $u_a = 5 \times 10^{-5} \text{ sr}^{-1}$ in (b).

validation data when fulfilling the necessary uncertainty requirements.

V. CONCLUSION

The performance of a scheme proposed for reconstructing hyperspectral R_{rs} from multispectral ones benefiting of a comprehensive dataset of simulated spectra, has been verified for PACE-OCI hyperspectral data in the 400–700 nm interval using R_{rs} at the AERONET-OC visible center-wavelengths. By exploiting in situ hyperspectral R_{rs} data representative of diverse water types, results obtained at PACE-OCI center-wavelengths of major interest for ocean color applications (identified as PACE-*m*), have shown mean relative differences between reconstructed and in situ hyperspectral R_{rs} values within $\pm 2\%$ across large portions of the visible spectrum for Case-1 and Case-2a water spectra and to a lesser extent for Case-2b spectra.

Benefiting of the former results, uncertainties exclusively due to the reconstruction of spectra have been quantified for each water type. The estimated relative uncertainties are generally lower than 2% up to 560 nm for Case-1 and Case-2a water spectra, and for Case-2b water spectra when also excluding the 450–480 and 520–550 nm spectral intervals. Acknowledging that an additional uncertainty due to the reconstruction of

hyperspectral R_{rs} constrained below approximately 1%–2% does not largely contribute to the overall uncertainty budget already characterizing experimental R_{rs} , results from this study support the validation of radiometric products from hyperspectral satellite sensors in large portions of the visible spectrum through the application of AERONET-OC multispectral data in combination with the proposed spectral reconstruction scheme and the considered simulated dataset.

ACKNOWLEDGMENT

The authors would like to thank the several colleagues who helped to deploy the Optical Floating System from the R/V Akademik during the 2016 BIO-OPT EUROFLEETS-2 cruise in the Black Sea, and from the R/V Minerva Uno during the 2017 SENTINEL3 cruise organized by the Italian National Research Council (CNR) in the Mediterranean Sea.

REFERENCES

- [1] C. R. McClain, “A decade of satellite ocean color observations,” *Annu. Rev. Mar. Sci.*, vol. 1, no. 1, pp. 19–42, Jan. 2009.
- [2] C. Donlon et al., “The global monitoring for environment and security (GMES) Sentinel-3 mission,” *Remote Sens. Environ.*, vol. 120, pp. 37–57, May 2012.
- [3] S. Cogliati et al., “The PRISMA imaging spectroscopy mission: Overview and first performance analysis,” *Remote Sens. Environ.*, vol. 262, Sep. 2021, Art. no. 112499.
- [4] P. J. Werdell et al., “The plankton, aerosol, cloud, ocean ecosystem mission: Status, science, advances,” *Bull. Amer. Meteorol. Soc.*, vol. 100, no. 9, pp. 1775–1794, Sep. 2019.
- [5] G. Zibordi et al., “Advances in the ocean color component of the aerosol robotic network (AERONET-OC),” *J. Atmos. Ocean. Technol.*, vol. 38, no. 4, pp. 725–746, Apr. 2021.
- [6] D. Vansteenwegen, K. Ruddick, A. Catrijssse, Q. Vanhellemont, and M. Beck, “The pan-and-tilt hyperspectral radiometer system (PANTHYS) for autonomous satellite validation measurements—Prototype design and testing,” *Remote Sens.*, vol. 11, no. 11, p. 1360, Jun. 2019.
- [7] M. R. Wernand, S. J. Shimwell, and J. C. De Munck, “A simple method of full spectrum reconstruction by a five-band approach for ocean colour applications,” *Int. J. Remote Sens.*, vol. 18, no. 9, pp. 1977–1986, Jun. 1997.
- [8] Z. Lee, S. Shang, C. Hu, and G. Zibordi, “Spectral interdependence of remote-sensing reflectance and its implications on the design of ocean color satellite sensors,” *Appl. Opt.*, vol. 53, no. 15, p. 3301, 2014.
- [9] B. C. Johnson et al., “Characterization and absolute calibration of an AERONET-OC radiometer,” *Appl. Opt.*, vol. 60, no. 12, p. 3380, 2021.
- [10] I. Cazzaniga and G. Zibordi, “AERONET-OC L_{WN} uncertainties: Revisited,” *J. Atmos. Ocean. Technol.*, vol. 40, no. 4, pp. 411–425, 2023.
- [11] G. Zibordi, “Experimental evaluation of theoretical sea surface reflectance factors relevant to above-water radiometry,” *Opt. Exp.*, vol. 24, no. 6, p. A446, 2016.
- [12] G. Zibordi, D. D’Alimonte, and T. Kajiyama, “Automated quality control of AERONET-OC L_{WN} data,” *J. Atmos. Ocean. Technol.*, vol. 39, no. 12, pp. 1961–1972, 2022.
- [13] P. J. Werdell, “PACE ocean color science data product requirements,” NASA, Goddard Space Flight Space Center Greenbelt, MD, USA, Tech. Rep., NASA/TM-2018—2018-219027, 2018.
- [14] M. Talone, G. Zibordi, and Z. Lee, “Correction for the non-nadir viewing geometry of AERONET-OC above water radiometry data: An estimate of uncertainties,” *Opt. Exp.*, vol. 26, no. 10, p. A541, May 2018.
- [15] J. Pitarch and V. Brando, “A hyperspectral and multi-angular bio-optical simulated dataset for global marine and inland water applications,” Istituto di Scienze Marine, Consiglio Nazionale delle Ricerche, ISMAR-CNR, 2024.